

Investigation of steric effects in inelastic collisions of NO($X^2\Pi$) with Ar

Millard H. Alexander^{a)}

Department of Chemistry and Biochemistry, University of Maryland, College Park, Maryland 20742-2021

Steven Stolte^{b)}

Laser Centre and Department of Physical Chemistry, Vrije Universiteit, De Boelelaan 1083, 1081 HV Amsterdam, The Netherlands

(Received 23 November 1999; accepted 8 February 2000)

Cross sections were determined for collisions of Ar with oriented NO($X^2\Pi$), based on full close-coupled calculations and new *ab initio* potential energy surfaces (PESs). Collisions in which the NO molecules are initially oriented so that the O end preferentially points toward the Ar atom are more effective in promoting spin-orbit changing transitions. The magnitude of the steric asymmetry is consistent with earlier calculations based on a previous PES, and agrees well with experiment. Various modifications of the full PESs were used to explore the origin of the observed features in the steric asymmetries, in particular the striking oscillatory pattern seen in the variation of the steric asymmetry with final state. © 2000 American Institute of Physics.

[S0021-9606(00)01017-5]

I. INTRODUCTION

Collisions involving molecular free radicals play a key role in chemical kinetics. These processes are complicated by the presence of electronic spin and/or orbital angular momentum, which can couple with the orbital angular momentum of the collision partners.¹ For collisions of molecules in a Π electronic state, two potential energy surfaces (PES's) are accessed during the collision.² From a semiclassical viewpoint, the underlying collision "trajectories" evolve simultaneously and coherently on the coupled PES's.³

As in other areas of physical chemistry, the greatest progress in the understanding of molecular reaction dynamics involving open-shell species comes from the detailed investigation of exemplary systems, which are simultaneously tractable by both theoreticians and experimentalists. For inelastic scattering, collisions of noble gases with NO have emerged as the paradigm.⁴ Experimental interest goes back nearly two decades^{5,6} and continues unabated to this day.⁷⁻¹³

In almost all of the prior experimental studies, both Λ -doublet (parity) levels of the lowest ($j = \Omega = 0.5$) rotation-spin-orbit level of NO were present initially. However, Stolte and co-workers have used an electric hexapole to prepare a beam of NO(X) solely in the upper Λ -doublet level.⁸ Scattering of this single state reveals^{8,14} oscillations in the magnitudes of the cross sections for scattering into particular final states, which are more pronounced than seen in scattering out of a statistical mixture of both Λ -doublet levels. More recently, Drabbels *et al.* used stimulated emission pumping to prepare a single rotational, Λ -doublet state in a vibrationally excited ($v = 20$) level of NO,¹⁵ which was then scattered by He.

In subsequent experiments Stolte and co-workers have

used a homogeneous electric field to orient state-selected NO molecules,^{9,12} so that either the "N" or "O" end of the molecule is preferentially pointed toward the Ar target. Similarly oriented beams of NO have been used in surface scattering experiments,¹⁶ which have been investigated theoretically by Lemoine and Corey.^{17,18} In closely related work, ter Meulen and co-workers have investigated^{19,20} the dependence on the orientation of cross sections for the scattering of OH, which also has a $^2\Pi$ electronic ground state.

The sensitivity of collisional inelasticity to the initial orientation of the NO (or OH) molecule is an additional probe of the underlying potential energy surface, which can complement or even extend the information furnished by conventional integral inelastic cross sections. Stolte, ter Meulen, and their co-workers^{9,12,19} report steric asymmetries for various inelastic transitions. These are defined as the difference between the inelastic cross section for an initial "heads" (NO) as opposed to an initial "tails" (ON) orientation, normalized by the sum of these two cross sections, and multiplied by 100 to convert the fraction to a percentage. For collisions of NO with Ar, the steric asymmetries are large and display a persistent alternation in sign as a function of the final state.¹²

Snijders and Bulthuis have used^{9,12} close-coupled calculations²¹ to determine the integral cross sections for the scattering of oriented NO molecules by Ar. The underlying expressions involve multiple summations over products of T -matrix elements and yield little direct insight into the underlying collisional propensities. To gain a better understanding of the origin and magnitude of the observed steric effects, we have advocated²² the determination first of differential cross sections for the scattering of an oriented molecule. Integral cross sections, and the steric asymmetries, can then be determined by integration over all scattering angles.

^{a)}Electronic mail: mha@mha-ibm4.umd.edu

^{b)}Electronic mail: stolte@chem.vu.nl

The investigation of Snijders and Bulthuis^{9,12} was based on our earlier ArNO PES's,¹⁴ determined with the coupled-electron-pair (CEPA) method.^{23,24} We have subsequently reported²⁵ more accurate PES's, determined with a larger atomic orbital basis set and a coupled-cluster treatment including the perturbative inclusion of triple excitations [CCSD(T)]. In the present paper we use these new CCSD(T) PES's to redetermine the magnitude of the Ar–NO steric asymmetries and to explore how the magnitude and sign of these steric asymmetries is governed by the PESs.

The organization of the present paper is as follows: In the next two sections we review briefly the scattering formalism and its application to collisions of oriented $^2\Pi$ molecules. In Secs. IV and V we then present calculated Ar–NO integral steric asymmetries and compare these with the experimental results of Stolte and co-workers.¹² The pronounced sign alternation of the steric asymmetries is investigated in Sec. VI. In Sec. VII we present the dependence of the differential scattering cross sections on the initial NO orientation. This is followed with a prediction of steric asymmetries in cross sections for spin–orbit changing transitions. We close with a brief discussion.

II. SCATTERING FORMALISM

We present here only those details that are directly pertinent to the present investigation; more complete information is available in several earlier publications.^{2,14,21,26,27} The rotational levels of a molecule in a $^2\Pi$ electronic state can be written as²⁸

$$|jm\Omega\varepsilon\Lambda\Sigma\rangle = 2^{-1/2} [|jm\Omega\rangle | \Lambda\Sigma\rangle + \varepsilon |jm-\Omega\rangle | -\Lambda-\Sigma\rangle]. \quad (1)$$

Here j denotes the total angular momentum of the diatomic molecule, with projections m and Ω along, respectively, the space- and molecule-fixed z -axes. Also $| \Lambda\Sigma\rangle$ designates the electronic component of the wave function, where Λ and Σ denote, respectively, the molecule-frame projections of the electronic orbital and spin angular momenta. The Λ - (or ‘parity’) doublet levels are distinguished by the symmetry index ε that can take the value $+1$ (e -labeled levels) or -1 (f -labeled levels).²⁹ The total parity of the wave functions is given by $\varepsilon(-1)^{j-\Omega}$.²⁹ For simplicity in what follows, we will suppress the electronic wave function $| \Lambda\Sigma\rangle$.

For the NO molecule, which is well described in Hund's case (a)²⁸ for all rotational levels that are accessed in the collision studies of Stolte and co-workers,^{9,12} Ω is a good quantum number. The $\Omega=0.5$ spin–orbit manifold lies lower in energy, so that the lowest rotational state is $j=\Omega=0.5$. For reference, for a given j the lower and higher in energy spin–orbit states are often designated F_1 and F_2 , respectively. So, for NO, the F_1 states correspond to $\Omega=0.5$ and the F_2 states, to $\Omega=1.5$.

The wave function for the ArNO system is expanded in a basis formed by taking products of the NO rotational-fine-structure wave functions of Eq. (1) multiplied by functions that describe the Ar–NO orbital rotation. The expansion coefficients are solutions to the standard close-coupled (CC) equations.

In terms of the fundamental T -matrix elements, calculated in a fully coupled basis,^{2,21,27} the scattering amplitude for a transition between two rotation-parity-projection states can be written as^{21,30}

$$\begin{aligned} f_{jm\Omega\varepsilon \rightarrow j'm'\Omega'\varepsilon'}(\hat{\mathbf{k}}') \\ = \pi^{1/2} \sum_{Jl'l'} (2l+1)^{1/2} (2J+1) i^{l-l'} \begin{pmatrix} j & J & l \\ m & -m & 0 \end{pmatrix} \\ \times \begin{pmatrix} j' & J & l' \\ m' & -m & m-m' \end{pmatrix} Y_{l',m,l'}(\hat{\mathbf{k}}') T^J(j'l'\Omega'\varepsilon',jl\Omega\varepsilon), \end{aligned} \quad (2)$$

where $(:::)$ is a Wigner $3j$ symbol³⁰ and the sum extends over all allowed values of the initial and final orbital angular momenta l and l' . In Eq. (2), \mathbf{k} and \mathbf{k}' indicate the initial and final collision wave vector. The direction of the initial wave vector $\hat{\mathbf{k}}$, which is also the direction of the initial relative velocity vector, defines the axis of m quantization in the so-called ‘collision frame.’ As defined by Eq. (12), the scattering amplitude is dimensionless, so that the differential cross section is given by

$$d\sigma_{jm\Omega\varepsilon \rightarrow j'm'\Omega'\varepsilon'}(\hat{\mathbf{k}}')/d\Omega = \frac{1}{k^2} |f_{jm\Omega\varepsilon \rightarrow j'm'\Omega'\varepsilon'}(\hat{\mathbf{k}}')|^2. \quad (3)$$

The approach of a structureless atom to a molecule in a $^2\Pi$ electronic state gives rise to two PES's, of A'' and A' symmetry with respect to reflection in the triatomic plane.² The PES's are a function of the three Jacobi coordinates used to describe the triatomic system: r (the NO bond distance), R (the distance between the Ar atom and the center of mass of the NO molecule), and θ (the angle between \mathbf{r} and \mathbf{R}), with $\theta=0$ corresponding to colinear ArNO. In both the sets of PESs,^{14,25} which we use here [CEPA and CCSD(T)], the NO bond distance was held fixed at its equilibrium value (1.15077 Å³¹).

In the treatment of the scattering, it is convenient to work with the average and half-difference of the PES's for the states of A'' and A' reflection symmetry, defined as²

$$V_{\text{sum}}(R, \theta) = 0.5 [V_{A''}(R, \theta) + V_{A'}(R, \theta)] \quad (4a)$$

and

$$V_{\text{dif}}(R, \theta) = 0.5 [V_{A''}(R, \theta) - V_{A'}(R, \theta)]. \quad (4b)$$

The dependence on θ is then expanded² in terms of reduced rotation matrix elements,³²

$$V_{\text{sum}}(R, \theta) = \sum_{\lambda=0}^{\lambda_{\text{max}}} V_{\lambda 0}(R) d_{00}^{\lambda}(\theta), \quad (5)$$

and

$$V_{\text{dif}}(R, \theta) = \sum_{\lambda=2}^{\lambda_{\text{max}}} V_{\lambda 2}(R) d_{20}^{\lambda}(\theta), \quad (6)$$

where the upper limit λ_{max} is imposed by the size of the angular grid on which *ab initio* points are available.^{14,25}

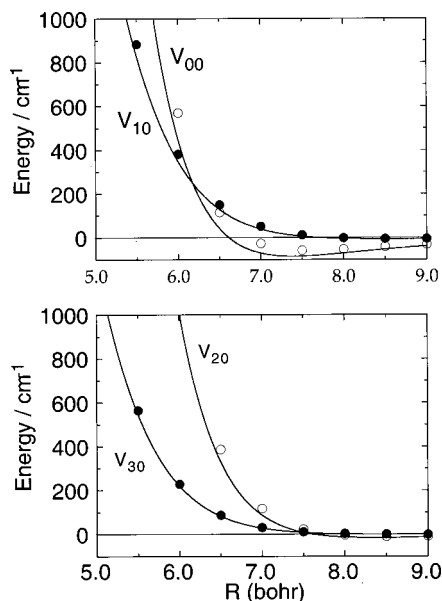


FIG. 1. A comparison of the dependence on the Ar–NO center-of-mass separation of the largest of the $V_{\lambda 0}(R)$ terms in the Legendre expansion of the sum PES [Eq. (5)], as predicted by our earlier CEPA calculations (circles, Ref. 14) and more recent CCSD(T) calculations (solid curves, Ref. 25).

Figures 1 and 2 present plots of the larger $V_{\lambda 0}(R)$ and $V_{\lambda 2}(R)$ terms in the expansion of the sum and difference potentials [Eqs. (5) and (6)], as determined by our earlier correlated electron pair (CEPA)^{23,24} and more recent coupled-cluster [CCSD(T)]³³ calculations. By far the largest difference in the two PES's appears in the isotropic ($\lambda=0$) component of the sum PES. Because the CCSD(T) calculations recover a larger fraction of the correlation energy, the well in the isotropic term, which is a manifestation of dis-

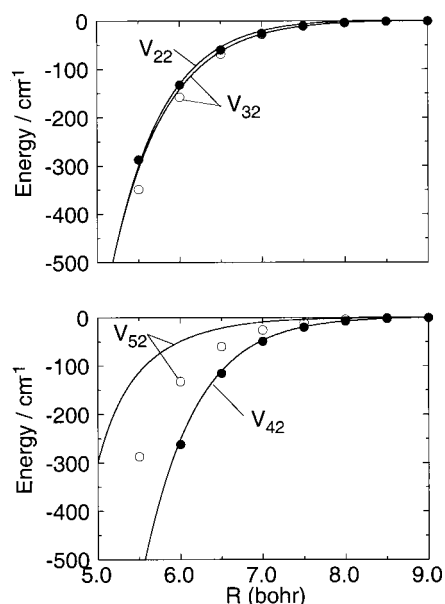


FIG. 2. A comparison of the dependence on the Ar–NO center-of-mass separation of the largest of the $V_{\lambda 2}(R)$ terms in the Legendre expansion of the difference PES [Eq. (6)], as predicted by our earlier CEPA calculations (circles, Ref. 14) and more recent CCSD(T) calculations (solid curves, Ref. 25).

person forces, is deeper than the well in the corresponding CEPA $V_{00}(R)$. The various anisotropic terms are extremely similar in both magnitude and dependence on R .

III. ORIENTED MOLECULE SCATTERING

A hexapole electric field state selector will focus the upper (f) Λ -doublet level of the NO molecule.^{8,34} If a static electric field (\vec{E}) is then imposed, this state will evolve into a linear combination of the field-free (e and f) states,^{9,19}

$$|jm\Omega\vec{E}\rangle = 2^{-1/2}[\alpha|jm\Omega e\rangle + \beta|jm\Omega f\rangle], \quad (7)$$

where the real coefficients α and β are given by solution of a 2×2 Stark mixing Hamiltonian.¹⁹ In the high-field limit, $|\alpha| = |\beta| = 1$; in general,

$$\alpha^2 + \beta^2 = 2. \quad (8)$$

Under the conditions of the experiments of Stolte and co-workers, when \vec{E} is parallel to the z axis, $|\alpha| = 0.785$ and $|\beta| = 1.176$.³⁵ The relative signs of α and β depend on the orientation of \vec{E} with respect to the Z -axis.^{9,19} For simplicity this will be suppressed hereafter, except where needed. The degree of orientation of the NO molecule that is prepared is given by⁹

$$\langle \cos \Theta \rangle = \alpha\beta \frac{m\Omega}{j(j+1)}, \quad (9)$$

where Θ is the angle of the NO molecular axis with respect to the electric field. Under the conditions of the Amsterdam group, the NO molecule is oriented so that in $\sim 75\%$ of collisions the N end points preferentially toward the Ar target.²² (The situation can be reversed by changing the direction of the electric field.)

For scattering of an oriented beam of NO molecules the appropriate scattering amplitude is

$$\begin{aligned} f_{jm\Omega\vec{E} \rightarrow j'm'\Omega'\epsilon'}(\hat{\mathbf{k}}') \\ = 2^{-1/2}[\alpha f_{jm\Omega e \rightarrow j'm'\Omega'\epsilon'}(\hat{\mathbf{k}}') + \beta f_{jm\Omega f \rightarrow j'm'\Omega'\epsilon'}(\hat{\mathbf{k}}')]. \end{aligned} \quad (10)$$

The corresponding oriented differential cross section $d\sigma_{j\Omega\vec{E} \rightarrow j'\Omega'\epsilon'}(\hat{\mathbf{k}}')$ is obtained by analogy with Eq. (4). In the experiments of Stolte, ter Meulen and their co-workers^{9,19} the hexapole field selects states corresponding to a definite sign of the product $m\Omega$. Since, in the scattering calculations, we use a definite-parity basis [Eq. (1)] in which both signed values of Ω appear, in the calculation of the oriented, differential cross sections we need to average over both values of $m = \pm|m|$. However, one can show that the square of Eq. (10) is unchanged when the initial and final projection quantum numbers (m, m') are replaced by their negatives ($-m, -m'$). Thus, we have

$$d\sigma_{j\Omega\vec{E} \rightarrow j'\Omega'\epsilon'}(\hat{\mathbf{k}}') = \sum_{m'} d\sigma_{jm\Omega\vec{E} \rightarrow j'm'\Omega'\epsilon'}(\hat{\mathbf{k}}'), \quad (11)$$

where m is a positive number. In the experiments of the Amsterdam group the hexapole state selected NO molecules are in $j = \frac{1}{2}$, so that one needs to consider only the single projection quantum number $m = \frac{1}{2}$. The expression for the

integral oriented cross sections is obtained by multiplying $d\sigma_{jm\Omega\vec{E}\rightarrow j'\Omega'\epsilon'}(\hat{\mathbf{k}}')$ by the sine of the angle and integrating over all scattering angles.

Following earlier notation,^{9,19} we will designate the differential, oriented-molecule cross sections as $d\sigma^{\text{NO}}(\hat{\mathbf{k}}')$ or $d\sigma^{\text{ON}}(\hat{\mathbf{k}}')$ depending on whether the direction of the electric field is chosen to orient preferentially the N or O end toward the Ar target. We shall hereafter suppress the indices $j\Omega\vec{E}\rightarrow j'\Omega'\epsilon'$, unless explicitly necessary. We shall use a similar superscript indexing for the integral oriented-molecule cross sections σ^{NO} and σ^{ON} . The dimensionless ‘‘steric asymmetry’’ is defined by⁹

$$100(\sigma^{\text{NO}} - \sigma^{\text{ON}})/(\sigma^{\text{NO}} + \sigma^{\text{ON}}). \quad (12)$$

From an examination of the underlying expression in terms of T -matrix elements, Stolte and co-workers⁹ have shown that the denominator of Eq. (12) is equal to

$$\sigma^{\text{NO}} + \sigma^{\text{ON}} = \alpha^2 \sigma_{j\Omega e \rightarrow j'\Omega'\epsilon'} + \beta^2 \sigma_{j\Omega f \rightarrow j'\Omega'\epsilon'}. \quad (13)$$

As the reader can readily show, this relation is also true at the level of the differential, oriented-molecule cross sections, namely,

$$d\sigma^{\text{NO}} + d\sigma^{\text{ON}} = \alpha^2 d\sigma_{j\Omega e \rightarrow j'\Omega'\epsilon'} + \beta^2 d\sigma_{j\Omega f \rightarrow j'\Omega'\epsilon'}. \quad (14)$$

Similarly, we find from Eqs. (7) and (10) that

$$d\sigma^{\text{NO}} - d\sigma^{\text{ON}} = 2\alpha\beta \sum_{m'} [f_{jme \rightarrow j'm'\Omega'\epsilon'}^*(\hat{\mathbf{k}}') \times f_{jmf \rightarrow j'm'\Omega'\epsilon'}(\hat{\mathbf{k}}') + \text{c.c.}], \quad (15)$$

where ‘‘c.c.’’ denotes the complex conjugate, and similarly to Eq. (11), the cross-section difference $d\sigma^{\text{NO}} - d\sigma^{\text{ON}}$ is independent of the sign of m .

IV. CALCULATED STERIC ASYMMETRIES

Stolte and co-workers reported close-coupled^{2,21,27} Ar–NO scattering calculations based on the CEPA PES at an initial collision energy of $E_{\text{col}} = 442 \text{ cm}^{-1}$ (0.0548 eV). To assess the effect of the differences between the CEPA and CCSD(T) PES's, we carried out full close-coupled calculations at this same energy, with both sets of PES's. The size of the rotational state expansion, as well as the integration parameters and maximum value of the total angular momentum J , were chosen^{14,36} to ensure an accuracy of better than 1% in the calculated T -matrix elements. All scattering calculations were based on the formalism we have developed,^{2,21,27} and performed with our HIBRIDON code.³⁷

The steric asymmetries calculated here with the CEPA PES's agree perfectly with those reported by Stolte and co-workers.¹² Since the latter calculations were done entirely differently, by means of a different scattering code (MOLSCAT³⁸ versus HIBRIDON³⁷), this agreement establishes the accuracy of both calculations.

Figure 3 compares the calculated steric asymmetries, determined with the CEPA and CCSD(T) PES's. We observe a generally excellent agreement, although there are substantial differences for $\Delta j \leq 4$ and $\Delta j \geq 12$. The most noticeable fea-

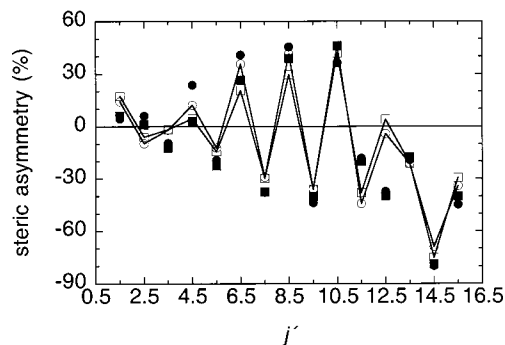


FIG. 3. A comparison of predicted steric asymmetries for inelastic collisions of oriented NO with Ar at a collision energy of 442 cm^{-1} . The figure refers to transitions into rotational levels of the $\Omega = 0.5(F_1)$ spin-orbit manifold. The electric field parameters α and β were set to the experimental values from Ref. 9: 0.785 and 1.176, respectively. The circles and squares designate, respectively, transitions into e and f -labeled Λ -doublet levels. The open symbols, linked by solid lines, indicate predictions based on the CCSD(T) PESs, while the filled symbols indicate predictions based on the CEPA PESs.

ture is the strong oscillation in the sign of the steric asymmetries, particularly for transitions with $5 \leq \Delta j \leq 11$. The oscillatory structure predicted by the CEPA and CCSD(T) PES's is very similar.

Before presenting the results of additional calculations, we prefer to make a few general observations, which are illustrated by Fig. 3. The only difference between the ‘‘NO’’ and ‘‘ON’’ oriented cross sections is the relative signs of α and β in Eq. (10).^{9,19} Thus the ‘‘NO’’ and ‘‘ON’’ oriented cross sections represent constructive and destructive quantum interference between the scattering out of the e and $f\Lambda$ -doublet levels. Consequently, and shown also by Eq. (15), $d\sigma^{\text{NO}} - d\sigma^{\text{ON}}$ will be largest if the amplitudes for scattering out of the e and $f\Lambda$ -doublet levels of the initial state are both significant in magnitude. If, for a given $j \rightarrow j'\epsilon'$ transition, the amplitude for either the $je \rightarrow j'\epsilon'$ or the $jf \rightarrow j'\epsilon'$ transition is small, then the steric asymmetry will be small.

For collisions of NO with Ar it is known^{8,22} that for spin-orbit conserving transitions with low Δj , the cross section is dominated by either e/f conserving or e/f changing processes. Thus, as predicted in the preceding paragraph, because of the large difference in magnitude between the $j\Omega e \rightarrow j'm'\Omega'\epsilon'$ and $j\Omega f \rightarrow j'm'\Omega'\epsilon'$ scattering amplitudes, we see in Fig. 3 that the steric asymmetries are small for low Δj , relative to those for large Δj .

In the pure Hund's case (a) limit,^{28,39} which is valid for NO at low j , the coupling between channels is independent of a reversal in the parity index of both the initial and final states.²¹ Thus, the coupling potential, and, consequently, the scattering amplitudes will display the following symmetries:²¹

$$f_{jme \rightarrow j'm'e} = f_{jmf \rightarrow j'm'f} \quad (16a)$$

and

$$f_{jme \rightarrow j'm'f} = f_{jmf \rightarrow j'm'e}. \quad (16b)$$

It follows from these results and Eq. (15) that for transitions into the two Λ -doublet levels (e and f) associated with a

given final rotational level, the sign of the steric asymmetry will be identical. This is also clear from Fig. 3, except, perhaps, for the steric asymmetry for the transition into the $j' = 12.5$ level. Here the steric asymmetries are both small, with one positive and the other negative.

V. COMPARISON WITH EXPERIMENT

Stolte and co-workers have just reported¹² a full set of experimentally determined steric asymmetries for inelastic but spin-orbit conserving collisions of NO with Ar. These values complete their earlier preliminary results.⁹ The recent experiments were carried out at a collision energy of 475 cm^{-1} (0.0589 eV), with a spread in energy of 214 cm^{-1} fwhm. For any given transition, the experimentally determined inelastic rate coefficient is⁴⁰

$$k = \int v \sigma(v) f(v) dv, \quad (17)$$

where v designates the collision velocity and $f(v)$ is the distribution of collision velocities in the experiment. In the Amsterdam experiments the parallel component of the collision velocity dominates over the perpendicular component, so that Eq. (17) becomes, after conversion from collision velocity to collision energy,

$$k = \left(\frac{2}{m}\right)^{1/2} \int f(E_{\text{col}}) \sigma(E_{\text{col}}) E_{\text{col}}^{1/2} dE_{\text{col}}. \quad (18)$$

To compare with experiment, we have carried out additional calculations with the CCSD(T) PESs at $E_{\text{col}} = 475 \text{ cm}^{-1}$ (the nominal experimental energy), as well as $E_{\text{col}} = 368$ and 582 cm^{-1} , which are the fwhm points. Using these cross sections and the values we had already calculated (Fig. 3) at $E_{\text{col}} = 442 \text{ cm}^{-1}$, and assuming that the distribution of collision energies $f(E_{\text{col}})$ is Gaussian, we approximate Eq. (18) by a four-point quadrature,

$$k = \left(\frac{2}{m}\right)^{1/2} \sum_{i=1}^4 e_i^{1/2} \sigma(E_i) \exp[-a(E_i - 475)^2] / \sum_{i=1}^4 \exp[-a(E_i - 475)^2], \quad (19)$$

where m is the Ar-NO collision reduced mass. The constant a is adjusted so that $f(E_{\text{col}})$ has the experimental fwhm, and here has the value 1.514×10^{-5} (for energies in wave number units).

Figure 4 compares the simulated steric asymmetries with the experimental values. The effect of the energy averaging is significant for rotationally inelastic transitions with $j' \geq 12.5$. As a consequence of their high internal energy, cross sections into these states increase dramatically with increasing E_{col} . Indeed, the $j' = 16.5$ level is not even energetically allowed at the nominal collision energy of 475 cm^{-1} . The overall agreement between experiment and theory is excellent, with several noticeable discrepancies: An overall trend is seen for the experimental steric asymmetries to be somewhat smaller in magnitude than the predicted values. This is particularly apparent for the lowest transition ($j = 0.5 \rightarrow 1.5$) and also for transitions into high final rotational levels (j'

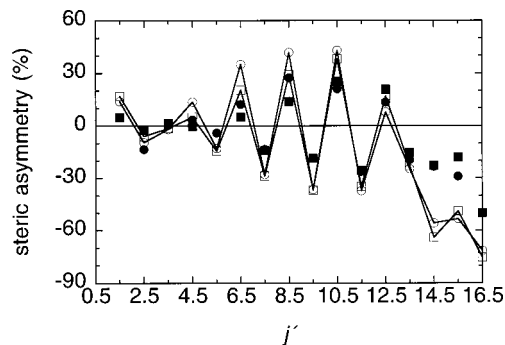


FIG. 4. Integral steric asymmetries for the scattering of NO by Ar. The circles and squares designate, respectively, transitions into e -labeled and f -labeled rotational levels of the $\Omega = 0.5(F_1)$ spin-orbit manifold. The open symbols, connected by solid lines, correspond to calculations based on the CCSD(T) PESs, averaged over a distribution of collision energies centered at $E = 475 \text{ cm}^{-1}$, with a fwhm of 214 cm^{-1} , while the filled symbols, unconnected by lines, correspond to the experimental values from Ref. 12.

≥ 14.5). Since the inelastic cross sections decrease in magnitude as Δj increases,²⁵ the precision of the experimental measurements may decrease for transitions into these high values of j' .

Overall, though, agreement with experiment is excellent. Particularly striking is the pronounced alternation in the sign of the steric asymmetry, which is positive for even Δj and negative for odd Δj . As can be seen in Fig. 3, this alternation is equivalently predicted by calculations based on the earlier CEPA PESs. In the next section we will focus on exploring the origin of this striking alternation. As will be seen, no clear explanation emerges of this striking alternation.

VI. DEPENDENCE OF THE STERIC ASYMMETRY ON FINAL ROTATIONAL STATE

To set the stage for further discussion, it will be worthwhile to review briefly some already known qualitative aspects of inelastic transitions involving molecules in $^2\Pi$ electronic states. For rotational-fine-structure states that are well described in the Hund's case (a) limit, transitions between states in the same spin-orbit manifold are induced primarily by the sum PES and transitions between states in different spin-orbit manifolds, primarily by the difference PES.

For collisions involving a molecule in a $^2\Pi$ electronic state, there will be no direct coupling between rotational levels j and j' unless^{2,8,21,27}

$$\varepsilon \varepsilon' (-1)^{j+j'+\lambda} = \varepsilon \varepsilon' (-1)^{\Delta j + \lambda + 1} = -1, \quad (20a)$$

and, further, unless

$$|j' - j| \leq \lambda \leq j + j'. \quad (20b)$$

Consequently, as discussed in detail by Werner and co-workers,⁴¹ when *even* terms dominate in the Legendre expansion of the PES, e/f conserving transitions ($\varepsilon' = \varepsilon$) will be stronger than e/f changing transitions for *even* Δj , while e/f changing transitions ($\varepsilon' = -\varepsilon$) will be stronger than e/f conserving transitions for *odd* Δj . In cases where the interaction potential is symmetric about $\theta = 90^\circ$, which would be the case for a homonuclear diatomic, all odd terms

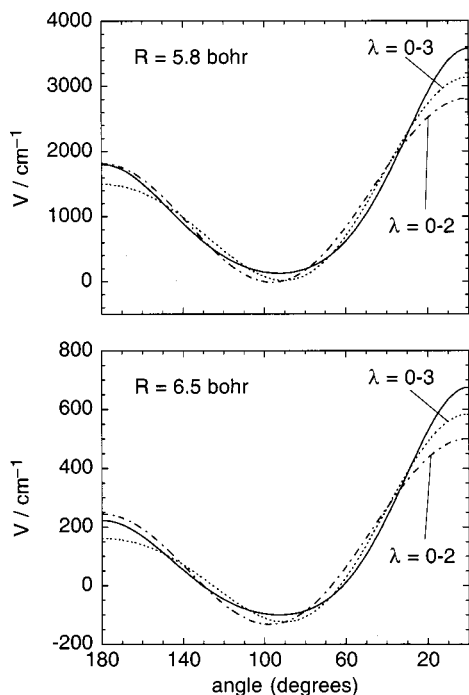


FIG. 5. Plot of the ArNO sum potential [Eq. (5)] as a function of the ArNO angle θ at two values of the Ar-NO center-of-mass separation. Note that $\theta=0$ corresponds to colinear ArNO. In both panels the solid curves correspond to the full set of Legendre expansion coefficients ($0 \leq \lambda \leq 9$), the short-dash curves correspond to retention of only the $\lambda=0-3$ expansion coefficients, and the long-dash-short-dash curves, to retention of only the $\lambda=0-2$ expansion coefficients.

in the Legendre expansion will vanish. If the system is “near homonuclear,” the odd terms will not vanish, but will be noticeably smaller than the even terms.

The classical turning point for Ar-NO collisions at $E = 475 \text{ cm}^{-1}$ is imposed by the spherically symmetric expansion term (V_{00}) in the expansion of V_{sum} and occurs at ~ 6 bohr. Outside of this point, the dominant expansion term in V_{sum} is V_{02} , as can be seen in Fig. 1. Because of this “near homonuclear” character there should occur a propensity toward e/f conservation for even Δj transitions, as discussed in the preceding paragraph. This has been seen both in earlier experimental work from the Stolte group⁸ as well as in our calculations.²⁵ It is most pronounced for the $j=0.5 \rightarrow 2.5$, 3.5, and 4.5 transitions ($\Delta j=2, 3$, and 4).^{8,25}

The “near-homonuclear” character of the potential is further illustrated by Fig. 5, which shows the angular dependence of the CCSD(T) $V_{\text{sum}}(R, \theta)$ for two values of R , 5.8 and 6.5 bohr. The first value corresponds to a point moderately high on the repulsive wall, with the second value somewhat farther out. Both points will be accessed in the experiments of Stolte and co-workers. The near symmetry about $\theta=90^\circ$ is apparent.

One is naturally tempted to inquire whether the strong alternation in the steric asymmetries seen in Figs. 3 and 4 is a consequence of the near-homonuclear character of the sum PES. As seen in Eq. (15), the difference in the “head” versus “tails” oriented-molecule cross sections is proportional to the product of the amplitudes for scattering into both the e and f/Λ -doublet levels of a particular final state. However, as

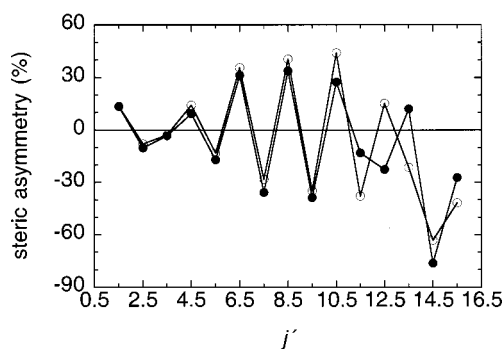


FIG. 6. Integral steric asymmetries for the scattering of NO by Ar at $E = 475 \text{ cm}^{-1}$ for scattering into e -labeled final rotational levels of the $\Omega = 0.5(F_1)$ spin-orbit manifold, from calculations based on our new CCSD(T) PESs. The open and filled circles designate, respectively, calculations based on the full PESs and calculations in which difference PES V_{dif} was set to zero.

encapsulated in Eq. (20), if even- λ terms dominate, then the scattering amplitude will be small for one or the other of final-state Λ -doublet levels. Thus we anticipate small steric asymmetries for transitions where the near-homonuclear propensity rules are the most pronounced. This prediction is most obvious for the $j=0.5 \rightarrow 2.5$ transition, where calculations with both sets of PESs as well as experiment yield small steric asymmetries (Figs. 3 and 4).

This result is not surprising, physically. The low Δj , spin-orbit conserving transitions are governed by the strong V_{20} term in the potential (Fig. 1). If the interaction potential is completely homonuclear, then the scattering will be independent of the heads/tails orientation of the molecule. Consequently, we anticipate small steric asymmetries for transitions for which the near homonuclearity is strongly apparent in the calculated integral cross sections.

To explore further the origin of the alternation in the steric asymmetries, we have carried out a series of additional calculations in which the CCSD(T) PESs were successively simplified. The first of these simplifications was to remove the V_{dif} PES. The predicted steric asymmetries at $E_{\text{col}} = 475 \text{ cm}^{-1}$ are shown in Fig. 6. Since the steric asymmetries are seen from Figs. 3 and 4 to be nearly independent of the e/f level of the final state, for clarity we only display in Fig. 6 (and in the subsequent figures) steric asymmetries for scattering into e -labeled final states.

We observe in Fig. 6 that the steric asymmetries are unaffected by the absence of the V_{dif} PES for all final states with $j' \leq 10.5$. As stated earlier, for a molecule in the Hund’s case (a) limit, scattering within a given spin-orbit manifold is governed only by the V_{sum} PES.²¹ However, as j increases the molecule becomes increasingly described in intermediate coupling,²⁸ so that the difference PES contributes increasingly to the scattering within the $\Omega = 0.5$ spin-orbit manifold, and, consequently, to the steric asymmetries. Comparison of Figs. 4 and 6 also suggests that the significant discrepancy between the experimental and theoretically predicted steric asymmetries for $j' > 12.5$ (see Fig. 4) might be attributed, at least partially, to residual inaccuracies in the difference PES.

We observe in Fig. 3 that significant differences between

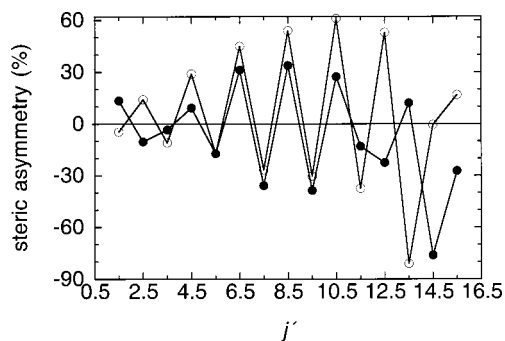


FIG. 7. Integral steric asymmetries for the scattering of NO by Ar at $E = 475 \text{ cm}^{-1}$ for scattering into e -labeled final rotational levels of the $\Omega = 0.5(F_1)$ spin-orbit manifold, from calculations based on our new CCSD(T) PESs. The filled and open circles designate, respectively, calculations based on the V_{sum} PESs and calculations in which all anisotropic terms in V_{sum} were damped to zero beyond the well in the isotropic term (see Fig. 1). In both cases the difference PES V_{dif} was set to zero.

the CEPA and CCSDT steric asymmetries occur for $j' \geq 10.5$. From the discussion in the preceding paragraph, we can likely attribute these differences to the known inaccuracies²⁵ in the CEPA V_{dif} .

Since we have now established that the steric asymmetries for $j' \leq 10.5$ are governed solely by the sum PES, we retain hereafter only the sum PES. The second simplification we shall make in the PES is the elimination of the long-range component in all the anisotropic expansion terms ($\lambda > 0$). This will allow the assessment of the relative role of the long-range attractive versus short-range repulsive part of the sum PES. To eliminate the long-range component of the anisotropy, we damp all $\lambda \neq 0$ terms in Eq. (5) rapidly to zero beyond the well in the spherically symmetric term by multiplication by the factor

$$\frac{1}{2}\{1 - \tanh[3(R - 6.845)]\}. \quad (21)$$

The calculated steric asymmetries are displayed in Fig. 7. We observe that the steric asymmetries most affected by the damping of the long-range component of the anisotropy in the PES are those for transitions with $\Delta j < 5$ and $\Delta j > 11$. We would certainly anticipate that the small Δj transitions, which involve the smallest changes in internal energy, would be sensitive to weak long-range forces. In addition, at large Δj , more than 50% of the initial translational energy is transferred into rotation. As pointed out first by Snijders and co-workers,¹² in this case the departing NO molecule will recede significantly slower. Consequently, its rotational motion will be more sensitive to weak long-range forces.

To explore further the sensitivity of the steric asymmetries on the deviation from the dominating homonuclear character (see Fig. 5), we have carried out two additional calculations, in which the range of Legendre terms in the expansion of V_{sum} [Eq. (4a)] was limited to $\lambda_{\text{max}} = 2$ and 3, respectively. [We recall that $\lambda_{\text{max}} = 9$ in the expansion of the CCSD(T) V_{sum} .] Since the expansion involves orthogonal polynomials, the low-order terms are unaffected by a reduction of λ_{max} . Figure 5 shows the angular dependence of these truncated potentials, for two values of R , and compares these to the angular dependence of the full V_{sum} . As can be seen,

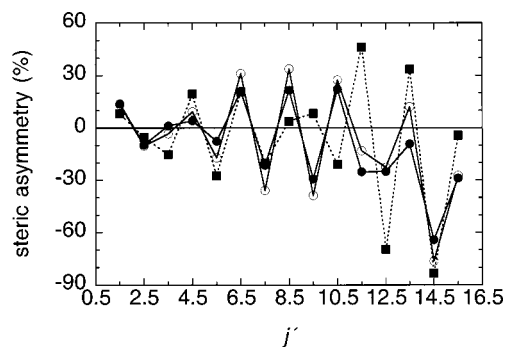


FIG. 8. Integral steric asymmetries for the scattering of NO by Ar at $E = 475 \text{ cm}^{-1}$ for scattering into e -labeled final rotational levels of the $\Omega = 0.5(F_1)$ spin-orbit manifold, from calculations based on our new CCSD(T) PESs. The open and filled circles, both connected by solid lines, and filled squares, connected by dashed lines, designate, respectively, calculations based on the V_{sum} PESs, calculations in which only the $\lambda = 0, 1, 2$, and 3 expansion terms in V_{sum} [Eq. (4a)] were retained, and calculations in which only the $\lambda = 0, 1$, and 2 terms in V_{sum} were retained.

truncation of the higher λ terms leads to some quantitative, but little qualitative, change in the potentials in the region of the classical turning point. In particular, the near-homonuclear character is well preserved.

The corresponding steric asymmetries, again just for transitions into e -labeled final states and at $E_{\text{col}} = 475 \text{ cm}^{-1}$, are shown in Fig. 8. For $\Delta j \leq 7$ the even-odd alternation is preserved in the calculations based on the truncated potentials. However, for larger Δj , the phase in the alternation is reversed, particularly for the when V_{sum} is truncated to $\lambda_{\text{max}} = 2$. This suggests that the finer details in the structure of the steric asymmetries, particularly for transitions with large Δj , cannot be explained fully by simple models of the ArNO interaction, even if they contain a good (but not completely accurate) description of the near-homonuclear character of the interaction potential.

VII. ORIENTATION DEPENDENCE OF DIFFERENTIAL CROSS SECTIONS

The steric asymmetries discussed above, and those measured in the experiments in Stolte's laboratory, are averages, over all scattering angles, of the differential oriented molecule cross sections [Eq. (11)]. The sign of the steric asymmetry is an indication of a greater efficiency of the N- or O-end approach in causing the particular transition in question. To examine whether this propensity is constant over all scattering angles, we plot in Fig. 9 the difference between the N- and O-end differential, oriented-molecule cross sections [Eq. (15)] for several representative transitions.

For small Δj ($j' = 1.5$ and 2.5), the major contribution to the steric asymmetry comes from forward scattering. Because inelastic forward scattering is due primarily to the long-range, attractive, anisotropic component of the PES, Fig. 9 helps to explain the observation (Sec. VI and Fig. 7) that the steric asymmetries for low Δj are most affected by the truncation of the long-range component of the anisotropy. We see in the lower panel of Fig. 9 that sideways scattering makes the major contribution to the observed oriented molecule cross sections for transitions with larger Δj .

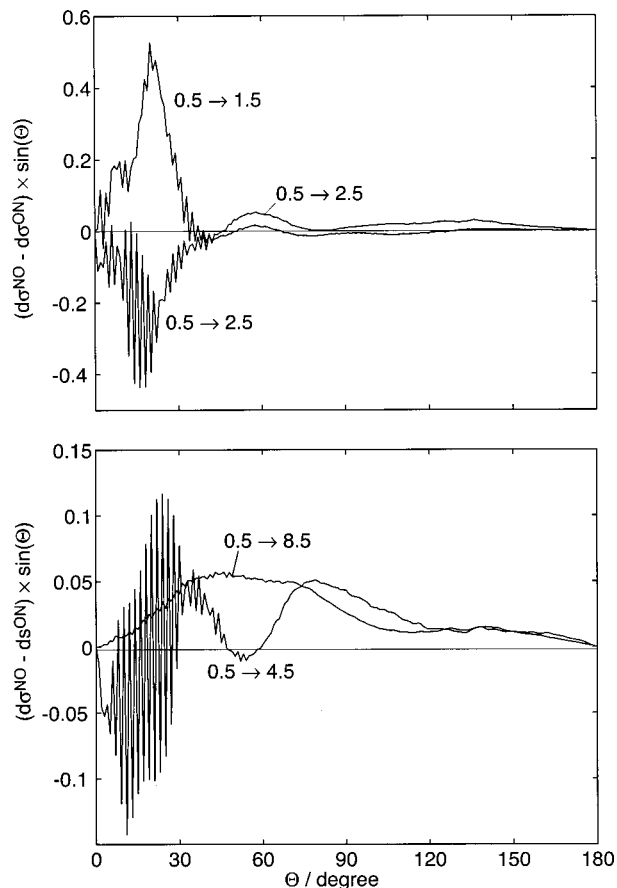


FIG. 9. The difference between the “heads” ($d\sigma^{\text{NO}}$) and “tails” ($d\sigma^{\text{ON}}$) differential cross sections for scattering out of the $j=0.5$, $\Omega=0.5$ level of NO into the $j'=1.5, 2.5, 4.5$, and 8.5 e -labeled rotational levels of the $\Omega=0.5$ spin-orbit manifold; $E=475\text{ cm}^{-1}$. In all cases, the differential, oriented-molecule cross sections have been weighted by the sine of the scattering angle. To avoid confusion with the Jacobi angle θ [Eqs. (3)–(6)], we use an upper case Θ to designate the center-of-mass scattering angle here.

The final, and important, observation from Fig. 9 is that (with the possible exception of the $j=0.5 \rightarrow j'=4.5$ differential cross section at small angle) the relative (heads versus tails) sizes of the oriented molecule cross sections appear to be little changed over the range of scattering angles which make the major contributions to the integral cross sections. Consequently, even if a particular experimental configuration is less sensitive to a range of scattering angles, little error will be introduced into the measured sign of the steric asymmetry.

VIII. STERIC ASYMMETRIES FOR SPIN-ORBIT CHANGING TRANSITIONS

Our focus in this article has been transitions within the $\Omega=0.5$ spin-orbit manifold, which correspond to the transitions that have been observed by Stolte and co-workers.¹² Cross sections for transitions into the $\Omega=1.5(F_2)$ spin-orbit manifold are weaker in magnitude, but nonetheless not negligible. Figure 10 compares cross sections out of the $\Omega=0.5$, $j=0.5, f$ level into j', f levels of the $\Omega=0.5$ spin-orbit manifold and into e and f levels of the $\Omega=1.5$ spin-orbit manifold. We observe that, for a given j' , the cross

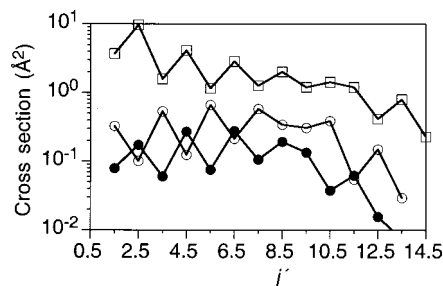


FIG. 10. Integral inelastic cross sections for the scattering out of the $j=0.5$, $\Omega=0.5, f$ level of NO by Ar at $E=475\text{ cm}^{-1}$, from calculations based on our new CCSD(T) PESs. The open squares designate spin-orbit conserving transitions into f -labeled final states of the $\Omega=0.5(F_1)$ spin-orbit manifold, while the open and filled circles designate, respectively, transitions into e - and f -labeled rotational levels of the $\Omega=1.5(F_2)$ spin-orbit manifold.

sections for spin-orbit-changing cross sections are roughly five to ten times smaller than for spin-orbit-conserving transitions. Despite this smaller magnitude we anticipate that increasing experimental sophistication will soon allow steric effects to be measured for spin-orbit changing transitions in collisions of NO.

To guide these future experiments, we present in Fig. 11 calculated steric asymmetries for Ar-NO $\Omega=0.5 \rightarrow 1.5$ transitions at $E=475\text{ cm}^{-1}$. As can be seen, there is considerable structure, although the steric asymmetries are negative for the most part. This indicates that O-end collisions are, overall, more effective in causing spin-orbit changing transitions. In addition, transitions into the $\Omega=1.5$ spin-orbit manifold no longer obey strictly the case (a) symmetry relations contained in Eq. (5). It is for this reason that transitions from low- j levels in the $\Omega=0.5$ spin-orbit manifold show a propensity^{7,11,14,25} for the population of Λ -doublet levels of A'' reflection symmetry⁴² (the e -labeled levels in the $\Omega=1.5$ spin-orbit manifold). It may be that this propensity, which is hardly apparent for transitions within the $\Omega=0.5$ spin-orbit manifold, is responsible for the observed difference (Fig. 11) between the steric asymmetries for transitions into e - and f -labeled final states, which is, overall, substantially larger than the difference seen (Fig. 3, for example) for transitions within the $\Omega=0.5$ spin-orbit manifold.

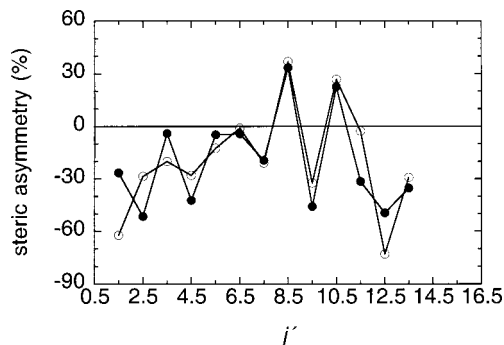


FIG. 11. Integral steric asymmetries for the scattering of NO by Ar at $E=475\text{ cm}^{-1}$ for spin-orbit changing transitions into final rotational levels of the $\Omega=1.5(F_2)$ spin-orbit manifold, from calculations based on our new CCSD(T) PESs. The open and filled circles designate, respectively, transitions into f - and e -labeled final states.

IX. DISCUSSION

The magnitude and sign of the steric asymmetry in the scattering of NO by Ar observed by Stolte and co-workers¹² are well predicted by calculations, based on both our earlier¹⁴ CEPA PESs and the more recent²⁵ CCSD(T) PESs. The most striking feature, present in both the theoretical predictions and the experimental observations, is a large oscillation in the sign of the steric asymmetry, which persists over nearly the entire range of Δj accessible at the experimental energy (475 cm⁻¹). For the spin-orbit conserving transitions, which were investigated experimentally, the steric asymmetry is nearly independent of the Λ -doublet symmetry (e/f) of the final state, which is consistent with the fact that NO at low to moderate j is well described in Hund's case (a). Model calculations were carried out, in which the CCSD(T) PES's were progressively truncated. These model studies indicate that (a) the most prominent features in the steric asymmetry are governed by the repulsive portion of the sum PES, and little affected by the weaker, long-range, attractive anisotropy or by the difference potential, and (b) the regularity of the alternation is not predicted by calculations in which the potential is truncated while preserving the "near-homonuclear" character.

On one hand, this last conclusion is disappointing, if one is seeking a simple explanation that attributes the observed alternation to the qualitative form of the PES. However, the sensitivity of the oscillatory structure to the higher-order, weak anisotropic terms shows clearly that observed steric asymmetries can provide a rigorous test of the accuracy of a calculated PES. As a corollary, the fact the both the CEPA and CCSD(T) PESs predict well the magnitude and phase of the observed steric asymmetries is a confirmation of the ability of current *ab initio* techniques to determine accurate PESs for the ArNO PESs.

The body of experimental evidence (see Ref. 25 for a recent summary) substantiates the accuracy of our *ab initio* calculations.^{14,25} of the sum ArNO PES. This is confirmed by the present calculations, where the good agreement shown in Fig. 4 for the spin-orbit conserving transitions, is, as we have seen in Sec. VI, insensitive to the difference PES. However, there is still some controversy²⁵ about the accuracy of the *ab initio* difference PES, which manifests itself primarily in spin-orbit changing transitions. The determination of steric asymmetries for inelastic, spin-orbit changing transitions of NO could well provide further experimental input into this question, as we have discussed in Sec. VIII.

The careful study of inelastic scattering involving oriented Π -state diatomic molecules can provide still more insight into the underlying potential energy surfaces. Recent studies,^{4,9,11} as well as the present work, demonstrate that the full interpretation and understanding of this type of experiment can be best achieved if coupled with high quality theoretical modeling, based on accurate potential-energy surfaces and a fully quantum treatment of the scattering dynamics. It is worthwhile emphasizing that the even ("homonuclear") terms in the Legendre expansion of the PES's [Eq. (5)] will not contribute to the steric asymmetry. Thus, the steric asymmetry is a unique probe of the odd Legendre terms—the deviation from homonuclearity. By

contrast, the overall inelastic cross sections—integral as well as differential—are sensitive to both the even and odd Legendre terms.

ACKNOWLEDGMENTS

M.H.A. is grateful to the U.S. National Science Foundation for partial support of this work under grant No. CHE-9971810. He would also like to thank Professor Jaap Snijders and Professor Jaap Bulthuis for communicating, prior to publication, the results of the calculations described in Ref. 12, Professor Hans ter Meulen for stimulating discussions, and the referee for helpful comments. S.S. is grateful to the Dutch Organization for Scientific Research, Nederlandse Organisatie voor Wetenschappelijk Onderzoek, for support under Fundamenteel Onderzoek Materie and Chemische Wetenschappen.

¹For a comprehensive recent review, see P. J. Dagdigian, in *Dynamics and Kinetics of Small Radicals*, edited by K. Liu and A. F. Wagner (World Scientific, Singapore, 1995), Part I, p. 315.

²M. H. Alexander, *Chem. Phys.* **92**, 337 (1985).

³G. Parlant and M. H. Alexander, *J. Chem. Phys.* **92**, 2287 (1990).

⁴P. L. James, I. R. Sims, I. W. M. Smith, M. H. Alexander, and M. Yang, *J. Chem. Phys.* **109**, 3882 (1998).

⁵A. S. Sudbø and M. M. T. Loy, *Chem. Phys. Lett.* **82**, 135 (1981); *J. Chem. Phys.* **76**, 2646 (1982).

⁶P. Andresen, H. Joswig, H. Pauly, and R. Schinke, *J. Chem. Phys.* **77**, 2204 (1982).

⁷C. R. Beiler, A. Sanov, and H. Reisler, *Chem. Phys. Lett.* **235**, 175 (1995).

⁸J. J. van Leuken, F. H. W. van Amerom, J. Bulthuis, J. G. Snijders, and S. Stolte, *J. Phys. Chem.* **99**, 15 573 (1995).

⁹J. J. van Leuken, J. Bulthuis, S. Stolte, and J. G. Snijders, *Chem. Phys. Lett.* **260**, 595 (1996).

¹⁰S. D. Jons, J. E. Shirley, M. T. Vonk, C. F. Giese, and W. R. Gentry, *J. Chem. Phys.* **105**, 5397 (1996).

¹¹A. Lin, S. Antonova, A. P. Tsakotellis, and G. C. McBane, *J. Phys. Chem.* **103**, 1198 (1999).

¹²M. J. L. de Lange, M. Drabbels, P. T. Griffiths, J. Bulthuis, S. Stolte, and J. G. Snijders, *Chem. Phys. Lett.* **313**, 491 (1999).

¹³T. Suzuki, *Faraday Discuss. Chem. Soc.* **113**, 484 (1999).

¹⁴M. H. Alexander, *J. Chem. Phys.* **99**, 7725 (1993).

¹⁵M. Drabbels, A. M. Wodtke, M. Yang, and M. H. Alexander, *J. Phys. Chem.* **101**, 6463 (1997).

¹⁶A. E. Wiskerke, C. A. Taatjes, A. W. Kleyn, R. J. W. E. Lahaye, S. Stolte, and A. Namiki, *J. Phys. Chem.* **95**, 8409 (1991), and references contained therein.

¹⁷G. C. Corey and D. Lemoine, *Chem. Phys. Lett.* **160**, 324 (1989).

¹⁸D. Lemoine and G. C. Corey, *J. Chem. Phys.* **94**, 767 (1991).

¹⁹K. Schreel and J. J. ter Meulen, *J. Phys. Chem. A* **101**, 7639 (1997).

²⁰M. C. van Beek and J. J. ter Meulen, abstracts *COMET XVI*, Assisi, IT, 1999, p. 166.

²¹M. H. Alexander, *J. Chem. Phys.* **76**, 5974 (1982).

²²M. H. Alexander, *Faraday Discuss. Chem. Soc.* **113**, 437 (1999).

²³W. Meyer, *Int. J. Quantum Chem., Symp.* **5**, 341 (1971).

²⁴W. Meyer, *J. Chem. Phys.* **58**, 1017 (1973).

²⁵M. H. Alexander, *J. Chem. Phys.* **111**, 7426 (1999).

²⁶T. Orlikowski and M. H. Alexander, *J. Chem. Phys.* **80**, 4133 (1984).

²⁷G. C. Corey and M. H. Alexander, *J. Chem. Phys.* **85**, 5652 (1986).

²⁸H. Lefebvre-Brion and R. W. Field, *Perturbations in the Spectra of Diatomic Molecules* (Academic, New York, 1986).

²⁹J. M. Brown *et al.*, *J. Mol. Spectrosc.* **55**, 500 (1975).

³⁰A. Arthurs and A. Dalgarno, *Proc. R. Soc. London, Ser. A* **256**, 540 (1960).

³¹K. P. Huber and G. Herzberg, *Molecular Spectra and Molecular Structure. IV. Constants of Diatomic Molecules* (Van Nostrand Reinhold, New York, 1979).

- ³²D. M. Brink and G. R. Satchler, *Angular Momentum*, 2nd ed. (Clarendon, Oxford, 1968).
- ³³P. J. Knowles, C. Hampel, and H.-J. Werner, *J. Chem. Phys.* **99**, 5219 (1993).
- ³⁴S. Stolte, in *Atomic and Molecular Beam Methods*, edited by G. Scoles (Oxford University Press, New York, 1988), Vol. 1.
- ³⁵The assignment of the values of α and β corrects a misprint in the title in Tables 1 and 2 of Ref. 9, as discussed in Ref. 22.
- ³⁶M. Yang and M. H. Alexander, *J. Chem. Phys.* **103**, 6973 (1995).
- ³⁷HIBRIDON is a package of programs for the time-independent quantum treatment of inelastic collisions and photodissociation written by M. H. Alexander, D. E. Manolopoulos, H.-J. Werner, and B. Follmeg, with contributions by P. F. Vohralik, D. Lemoine, G. Corey *et al.* More information and/or a copy of the code can be obtained from the website <http://www-mha.umd.edu/~mha/hibridon>.
- ³⁸J. M. Hutson and S. Green, MOLSCAT computer code, version 14, 1994, distributed by Collaborative Computational Project No. 6 of the Engineering and Physical Sciences Research Council, United Kingdom.
- ³⁹G. Herzberg, *Spectra of Diatomic Molecules*, 2nd ed. (Van Nostrand, Princeton, 1968).
- ⁴⁰I. W. M. Smith, *Kinetics and Dynamics of Elementary Gas Reactions* (Butterworths, London, 1980).
- ⁴¹A. Degli-Esposti, A. Berning, and H.-J. Werner, *J. Chem. Phys.* **103**, 2067 (1995), and references contained therein.
- ⁴²M. H. Alexander *et al.*, *J. Chem. Phys.* **89**, 1749 (1988).